OPEN

see commentary on page 437

Rictor/mTORC2 signaling mediates TGFβ1-induced fibroblast activation and kidney fibrosis

Jianzhong Li[1], Jiafa Ren[1], Xin Liu[1], Lei Jiang[1], Weichun He[1], Weiping Yuan[2], Junwei Yang[1] and Chunsun Dai[1,3]

[1]Center for Kidney Disease, Second Affiliated Hospital, Nanjing Medical University, Nanjing, Jiangsu, China; [2]State Key Laboratory of Experimental Hematology, Institute of Hematology and Blood Disease Hospital, Chinese Academy of Medical Science and Peking Union Medical College, Tianjin, China and [3]State Key Laboratory of Reproductive Medicine, Institute of Toxicology, Nanjing Medical University, Nanjing, Jiangsu, China

The mammalian target of rapamycin (mTOR) was recently identified in two structurally distinct multiprotein complexes: mTORC1 and mTORC2. Previously, we found that Rictor/mTORC2 protects against cisplatin-induced acute kidney injury, but the role and mechanisms for Rictor/mTORC2 in TGFβ1-induced fibroblast activation and kidney fibrosis remains unknown. To study this, we initially treated NRK-49F cells with TGFβ1 and found that TGFβ1 could activate Rictor/mTORC2 signaling in cultured cells. Blocking Rictor/mTORC2 signaling with Rictor or Akt1 small interfering RNAs markedly inhibited TGFβ1-induced fibronection and α-smooth muscle actin expression. Ensuing western blotting or immunostaining results showed that Rictor/mTORC2 signaling was activated in kidney interstitial myofibroblasts from mice with unilateral ureteral obstruction. Next, a mouse model with fibroblast-specific deletion of Rictor was generated. These knockout mice were normal at birth and had no obvious kidney dysfunction or kidney morphological abnormality within 2 months of birth. Compared with control littermates, the kidneys of Rictor knockout mice developed less interstitial extracellular matrix deposition and inflammatory cell infiltration at 1 or 2 weeks after ureteral obstruction. Thus our study suggests that Rictor/mTORC2 signaling activation mediates TGFβ1-induced fibroblast activation and contributes to the development of kidney fibrosis. This may provide a therapeutic target for chronic kidney diseases.

Kidney International (2015) **88,** 515–527; doi:10.1038/ki.2015.119; published online 13 May 2015

KEYWORDS: cell signaling; fibroblast; fibrosis

Correspondence: *Chunsun Dai, The Center for Kidney Disease, Second Affiliated Hospital, Nanjing Medical University, 262 North Zhongshan Road, Nanjing, Jiangsu 210003, China. E-mail: daichunsun@njmu.edu.cn*

Received 16 August 2014; revised 23 February 2015; accepted 26 February 2015; published online 13 May 2015

Kidney interstitial fibrosis is one of the major pathological features for chronic kidney diseases. Fibroblasts in the kidneys have an essential role in maintaining the homeostasis of interstitial matrix and adjacent tissue under physiological condition. Although all cell types in the kidneys are involved in the pathogenesis of kidney fibrosis, fibroblasts which acquire the phenotype of myofibroblast and generate a large amount of interstitial matrix upon activation are the principal matrix-producing cells.[1–4]

The 'target of rapamycin' (TOR) is a serine/threonine kinase that controls cell metabolism, growth, proliferation, survival, and aging. Mammalian TOR kinase (mTOR) exists in two structurally and functionally distinct protein complexes, named mTOR complex 1 (mTORC1) and mTOR complex 2 (mTORC2).[5–7] A number of studies demonstrated that mTORC1 signaling has an important role in several forms of kidney disease.[8–12] Our and the other's studies report that mTORC1 signaling is linked to the fibrogenic process through promoting fibroblast activation.[13,14] MTORC2 consists of mTOR kinase, Rictor, mSIN1, Protor, mLST8, and DEPTOR. Among them, Rictor, acting as a scaffold protein, facilitates both the assembly of mTORC2 and the interaction of mTORC2 with its substrates and regulators. Ablation of Rictor diminishes mTORC2 signaling. MTORC2 may control cell survival, actin cytoskeleton organization, and other processes through phosphorylating several members of the AGC kinase family, including Akt, SGK1, and protein kinase C (PKC).[6,7,15–19] Our previous study reports that Rictor/mTORC2 signaling is crucial for protecting against cisplatin-induced tubular epithelial cell death.[20] MTORC2 pathway is reported to be an essential downstream branch of TGFβ1 signaling and represents a responsive target to inhibit cancer cell epithelial-to-mesenchymal transition.[21] Blocking mTORC2 signaling with MLN0128, an active site dual mTOR inhibitor, could largely inhibit TGFβ1-induced lung fibroblast activation and lung fibrosis.[22] Together, it is highly possible that Rictor/mTORC2 signaling have an important role in mediating TGFβ1-induced renal fibroblast activation and kidney fibrosis.

In this study, we found that TGFβ1 could induce Rictor/mTORC2 signaling activation in NRK-49F cells, and blocking this signaling inhibited TGFβ1-induced fibroblast activation. Mice with fibroblast-specific deletion of Rictor are phenotypic normal, and less kidney fibrosis could be detected in the knockout kidneys compared with those in the control littermates after unilateral ureter obstruction (UUO).

RESULTS

TGFβ1 induces Rictor/mTORC2 signaling activation in NRK-49F cells

NRK-49F cells, a rat kidney interstitial fibroblast cell line, were treated with TGFβ1 (2 ng/ml) for different time duration and dosage as indicated. As shown in Figure 1a and b, Rictor expression was induced at as early as 15 min, reached peak from 0.5 to 6 h and declined at 12 h after treatment. Following the induction of Rictor, the abundance of p-Akt (Ser473) began to increase at 3 h and reached peak from 6 to 24 h. Phosphorylated SGK1 was induced at a similar pattern with p-Akt (Ser473). The p-Akt (Thr308) abundance was continuously increased within 48 h after TGFβ1 treatment. NRK-49F cells were also treated with TGFβ1 at different dosage as indicated and harvested at 6 h after treatment. The western blotting analyses revealed that TGFβ1 could upregulate Rictor, p-Akt (Ser473), and p-Akt (Thr308) expression in a dose-dependent manner (Figure 1c). Immunofluorescent staining results showed that Rictor protein was increased in NRK-49F cells and mainly located in the cytosol at 6 h after TGFβ1 treatment (Figure 1d). TGFβ1 could induce the expression of Rictor mRNA at 0.5 and 1 h after treatment (Figure 1e). Together, it is concluded that TGFβ1 may activate mTORC2 signaling in kidney fibroblasts.

Rictor/mTORC2 signaling activation mediates TGFβ1-induced fibroblast activation

The role for Rictor/mTORC2 signaling in TGFβ1-induced fibroblast activation was then investigated. NRK-49F cells were transfected with scramble or Rictor small interfering

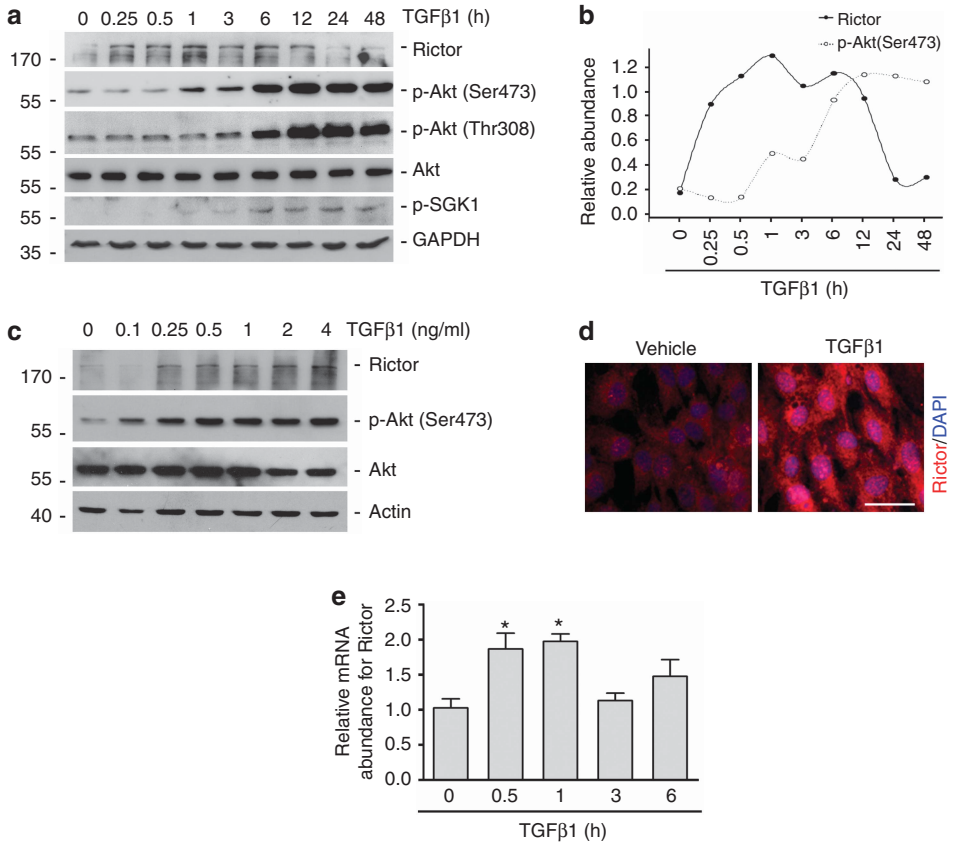

Figure 1 | Transforming growth factor β1 (TGFβ1) induces Rictor/mammalian target of rapamycin complex 2 (mTORC2) signaling activation in NRK-49F cells. NRK-49F cells were treated with TGFβ1 for different time or dosage as indicated. (**a–c**) Western blotting analyses showing the induction and activation of Rictor/mTORC2 signaling after TGFβ1 treatment in a time- (**a**, **b**) and dose-dependent (**c**) manner. Cell lysates were immunoblotted with Abs against Rictor, p-Akt (Ser473), p-Akt (Thr308), Akt, p-SGK1, and glyceraldehyde 3-phosphate dehydrogenase (GAPDH), respectively. (**b**) Graphic presentation showing the changes for the Rictor and p-Akt (Ser473) normalized to GAPDH and Akt, respectively. (**d**) Representative micrographs of immunofluorescent staining showing the induction of Rictor in NRK-49F cells after TGFβ1 treatment. Cells were co-stained with DAPI (4,6-diamidino-2-phenylindole) to visualize the nuclei. Scale bar = 10 μm. (**e**) The graph showing the results of Rictor mRNA abundance by the real-time PCR analysis. *$P < 0.05$ compared with control ($n = 4$).

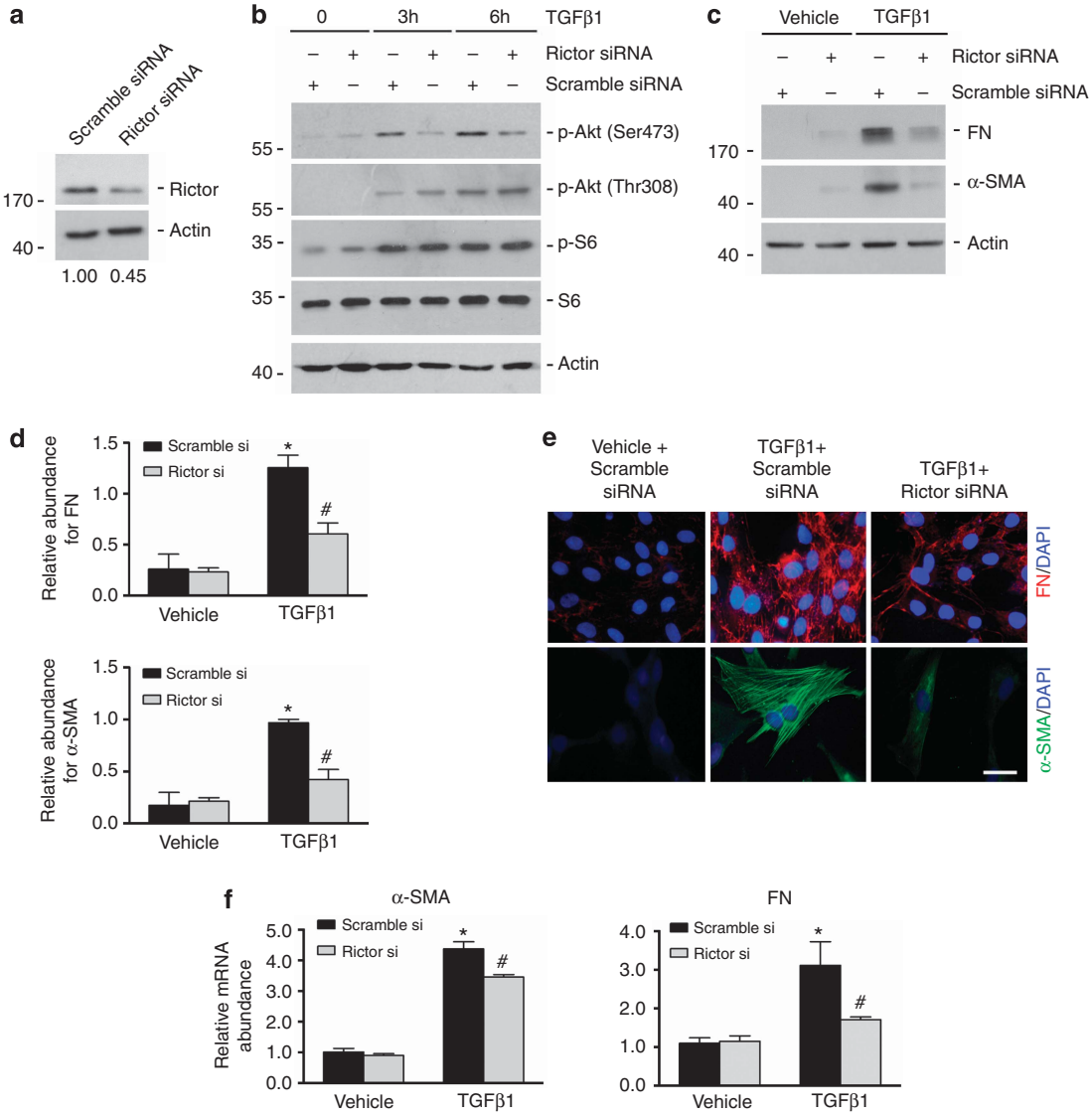

Figure 2 | Knocking down Rictor expression diminishes transforming growth factor β1 (TGFβ1)-induced Akt phosphorylation as well as fibroblast activation. NRK-49F cells were pretreated with scramble or Rictor small interfering RNA (siRNA) for 24 h, followed by TGFβ1 treatment for different time as indicated. (**a**) Western blotting analyses revealing the downregulation of Rictor protein in NRK-49F cells at 24 h after Rictor siRNA transfection. The relative abundance of Rictor protein was listed under the image. (**b**) Western blotting analyses showing that knocking down Rictor blocked TGFβ1-induced Akt phosphorylation at Ser473. The abundance of Akt phosphorylation at Thr308 as well as p-S6 was not changed in the cells transfected with Rictor siRNA. Cell lysates were immunoblotted with Abs against p-Akt (ser473), p-Akt (Thr308), Akt, p-S6, S6, and Actin, respectively. (**c**) Western blotting analyses showing that knocking down Rictor inhibited fibronectin (FN) and α-smooth muscle actin (α-SMA) expression at 48 h after TGFβ1 treatment. (**d**) Graphic presentation for FN and α-SMA protein expression in NRK-49F cells. $^*P<0.05$ compared with controls ($n=3$); $\#P<0.05$ compared with TGFβ1-treated cells ($n=3$). (**e**) Representative micrographs showing the immunostaining for FN and α-SMA after various treatments as indicated. NRK-49F cells were transfected with scramble or Rictor siRNA and then incubated with TGFβ1 (2 ng/ml) for 48 h. Cells were co-stained with DAPI (4,6-diamidino-2-phenylindole) to visualize the nuclei. Scale bar = 10 μm. (**f**) The graph showing the results of α-SMA and FN mRNA abundance after TGFβ1 treatment. $^*P<0.05$ compared with vehicle control ($n=4$), $\#P<0.05$ compared with those cells treated with scramble siRNA transfection and TGFβ1 ($n=4$).

RNA (siRNA). As shown in Figure 2a, at 24 h after transfection, Rictor protein expression was downregulated about 55% in cells transfected with Rictor siRNA compared with those transfected with scramble siRNA. To investigate the role for Rictor on TGFβ1-induced Akt phosphorylation, NRK-49F cells transfected with scramble or Rictor siRNA were treated with TGFβ1 for 3 and 6 h. As shown in Figure 2b, TGFβ1 treatment could largely increase p-Akt (Ser473), p-Akt (Thr308), and p-S6 abundance in cells transfected with scramble siRNA, whereas in Rictor siRNA-transfected cells, the abundance for p-Akt (Ser473) but not p-Akt (Thr308) or p-S6 was largely diminished, suggesting that the induction of p-Akt (Ser473) was dependent on Rictor in NRK-49F cells. To further determine the induction of

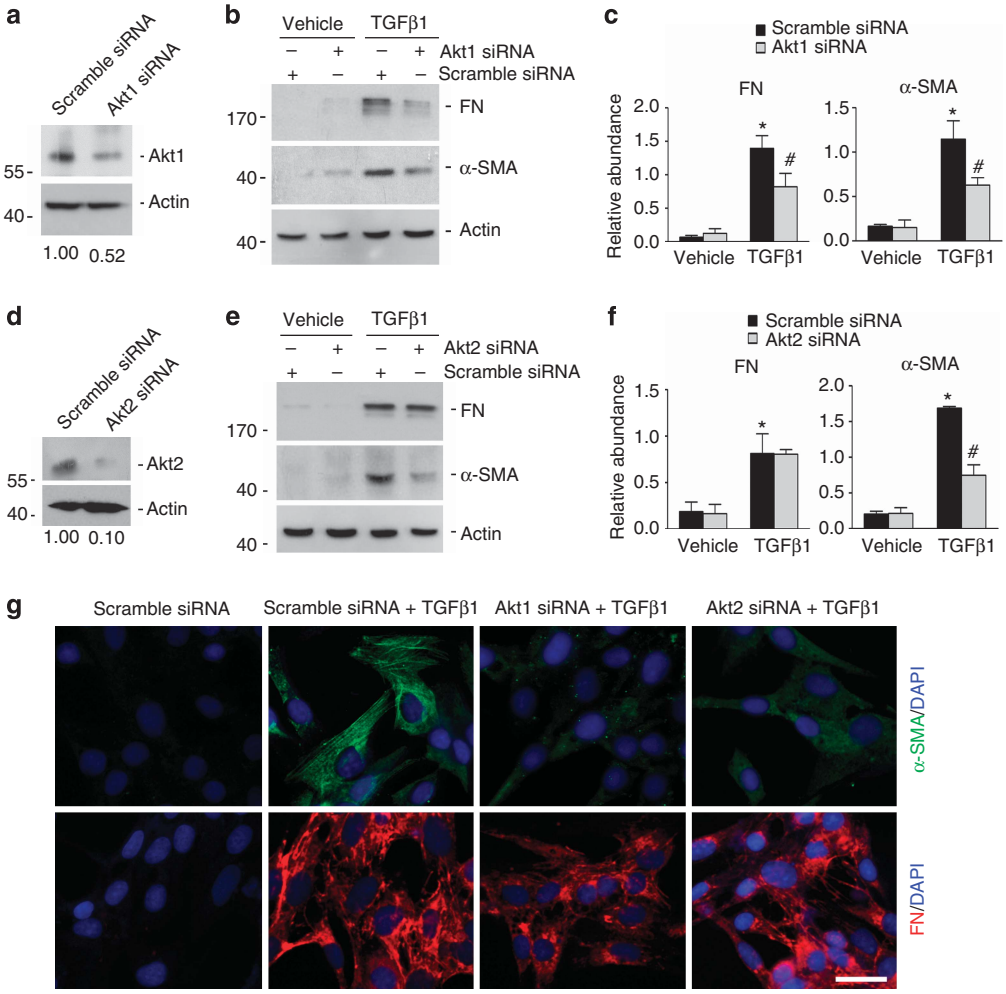

Figure 3 | Knocking down Akt diminishes transforming growth factor β1 (TGFβ1)-induced fibroblast activation. NRK-49F cells were pretreated with scramble, Akt1, or Akt2 small interfering RNA (siRNA) for 24 h, followed by TGFβ1 (2 ng/ml) treatment. (**a**, **d**) Western blotting analyses demonstrating the downregulation of Akt1 (**a**) or Akt2 (**d**) after siRNA transfection, respectively. (**b**) Western blotting analyses showing that knocking down Akt1 inhibited TGFβ1-induced fibronectin (FN) and α-smooth muscle actin (α-SMA) expression in NRK-49F cells. Cell lysates were immunoblotted with Abs against FN, α-SMA, and Actin, respectively. (**c**) Graphic presentation for FN and α-SMA protein expression in NRK-49F cells administered with scramble or Akt1 siRNA and followed by TGFβ1 treatment. $^{*}P<0.05$ compared with controls ($n=3$); $^{\#}P<0.05$ compared with TGFβ1-treated cells ($n=3$). (**e**) Western blotting analyses showing that knocking down Akt2 could inhibit TGFβ1-induced α-SMA expression at 48 h after treatment. (**f**) Graphic presentation for FN and α-SMA protein abundance. $^{*}P<0.05$ compared with controls ($n=3$); $^{\#}P<0.05$ compared with TGFβ1-treated cells ($n=3$). (**g**) Representative micrographs showing the immunostaining for FN and α-SMA. Cells were co-stained with DAPI (4,6-diamidino-2-phenylindole) to visualize the nuclei. Scale bar = 10 μm.

Rictor on TGFβ1-induced fibroblast activation, NRK-49F cells transfected with different sets of the siRNA were treated with TGFβ1 (2 ng/ml) for 48 h. As shown in Figure 2c and d, TGFβ1 could remarkably induce fibronectin (FN) and α-smooth muscle actin (α-SMA) expression in scramble siRNA-transfected cells, while Rictor siRNA transfection could markedly decrease their expression. Immunofluorescent staining further confirmed western blotting results for FN and α-SMA in NRK-49F cells (Figure 2e). We also detected the mRNA abundance of FN and α-SMA in NRK-49F cells by real-time PCR assay. The induction of FN and α-SMA mRNA expression after TGFβ1 treatment was decreased in Rictor siRNA-transfected cells (Figure 2f). Knocking down Rictor could not affect Smad3 phosphorylation induced by TGFβ1 treatment, suggesting that the profibrotic role of Rictor in fibroblast is independent of Smad3 phosphorylation (Supplementary Figure S1).

Akt1 and Akt2 but not Akt3 mRNA are expressed in the kidneys,[23] and mTORC2 is able to regulate the activity of both Akt1 and Akt2.[24,25] To decipher the role for Akt in TGFβ1-Induced fibroblast activation, NRK-49F cells were transfected with scramble, Akt1 or Akt2 siRNA. As shown in Figure 3a and d, Akt1 or Akt2 siRNA transfection could markedly downregulate Akt1 or Akt2 protein expression, respectively, compared with those transfected with scramble siRNA. NRK-49F cells were transfected with different sets of siRNA for 24 h, followed by TGFβ1 treatment for 48 h. Similar to Rictor siRNA transfection, Akt1 siRNA transfection could

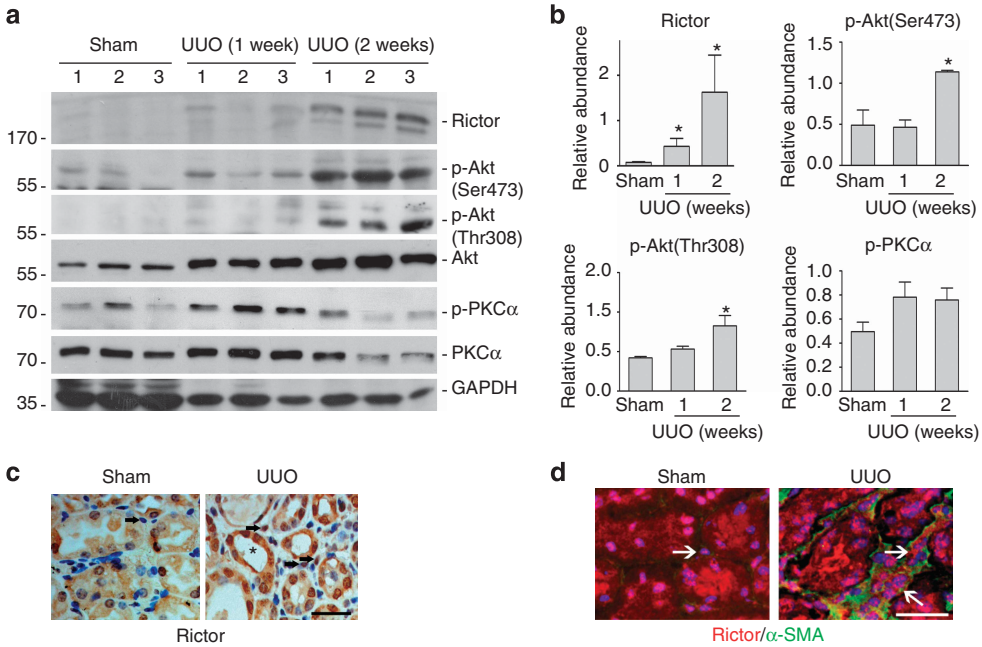

Figure 4 | Activation of Rictor/mammalian target of rapamycin complex 2 (mTORC2) signaling in the interstitial myofibroblasts from fibrotic kidneys. (**a**) Western blotting analyses showing the induction of Rictor, p-Akt (Ser473), p-Akt (Thr308), and phosphorylated protein kinase Cα (p-PKCα) in the kidneys with unilateral ureter obstruction (UUO) nephropathy compared with sham control. Kidneys were collected at day 7 and 14 after UUO. Kidney tissue lysates were immunoblotted with Abs against Rictor, p-Akt (Ser473), p-Akt (Thr308), Akt, p-PKCα, PKCα, and glyceraldehyde 3-phosphate dehydrogenase (GAPDH), respectively. Numbers (1–3) indicate each individual animal in a given group. (**b**) Graphic presentation showing the relative abundance for Rictor, p-Akt (Ser473), p-Akt (Thr308), and p-PKCα normalized to Akt and PKCα, respectively. *$P<0.05$ compared with sham controls ($n=3$). (**c**) Representative micrographs showing the immunostaining results for Rictor in the kidneys at day 14 after UUO. Kidney sections from the sham and UUO mice were immunostained with antibody against Rictor. Black arrows indicate interstitial cells. Asterisk indicates the tubule. Scale bar = 20 μm. (**d**) Representative micrographs showing immunostaining results for Rictor and α-SMA in the kidneys at day 14 after UUO. Kidney sections from the sham and UUO mice were co-stained with Abs against Rictor and α-SMA. Slides were counterstained with DAPI (4,6-diamidino-2-phenylindole) to visualize cell nuclei. White arrows indicate the interstitial cells. Scale bar = 20 μm.

markedly downregulate TGFβ1-induced FN and α-SMA expression (Figure 3b and c). However, Akt2 siRNA transfection could only significantly decrease α-SMA expression induced by TGFβ1 treatment (Figure 3e and f). Immunofluorescent staining further confirmed the results of western blotting assay (Figure 3g). The mRNA abundance for α-SMA and FN in the cells transfected with Akt1 siRNA was also significantly downregulated compared with those transfected with scramble siRNA at 24 h after TGFβ1 treatment (Supplementary Figure S2). Thus it is clear that Rictor/mTORC2/Akt signaling activation has an important role in mediating TGFβ1-induced fibroblast activation.

Rictor/mTORC2 signaling is activated in myofibroblasts from fibrotic kidneys

The activation of Rictor/mTORC2 signaling in myofibroblasts was further investigated in the fibrotic kidneys from mice with UUO nephropathy. Similar to the previous report,[26] the UUO kidneys developed severe interstitial fibrosis at 7 and 14 days after operation (data not shown). Western blotting analysis was employed to identify the activation of mTORC2 signaling. As shown in Figure 4a, pronounced induction of Rictor protein and p-Akt (ser473) was detected in the fibrotic kidneys at 7 and 14 days after UUO. To identify the cell types in which Rictor was induced, an immunohistochemical staining for Rictor was deployed. As shown in Figure 4c, the staining for Rictor protein was weak in both tubular cells and interstitial cells from the sham kidneys. However, in UUO kidneys, the staining for Rictor was markedly enhanced in both tubular cells and interstitial cells. The kidney sections were then co-stained with antibodies against α-SMA and Rictor to further identify the expression of Rictor in myofibroblasts in the UUO kidneys. The results showed that very weak expression for α-SMA or Rictor was detected in the interstitial cells from the sham kidneys, while in the UUO kidneys the induction of Rictor in α-SMA-positive cells could be detected, suggesting the induction of Rictor in myofibroblasts in the UUO kidneys. Thus these results suggest that Rictor/mTORC2 signaling is activated in the myofibroblasts from the fibrotic kidneys with UUO nephropathy.

Generation of mice with fibroblast-specific deletion of Rictor

To further explore the role of Rictor/mTORC2 signaling in fibroblast activation and kidney fibrosis *in vivo*, we generated a mouse model with fibroblast-specific deletion of Rictor gene by utilizing the Cre-LoxP system. Figure 5a shows the

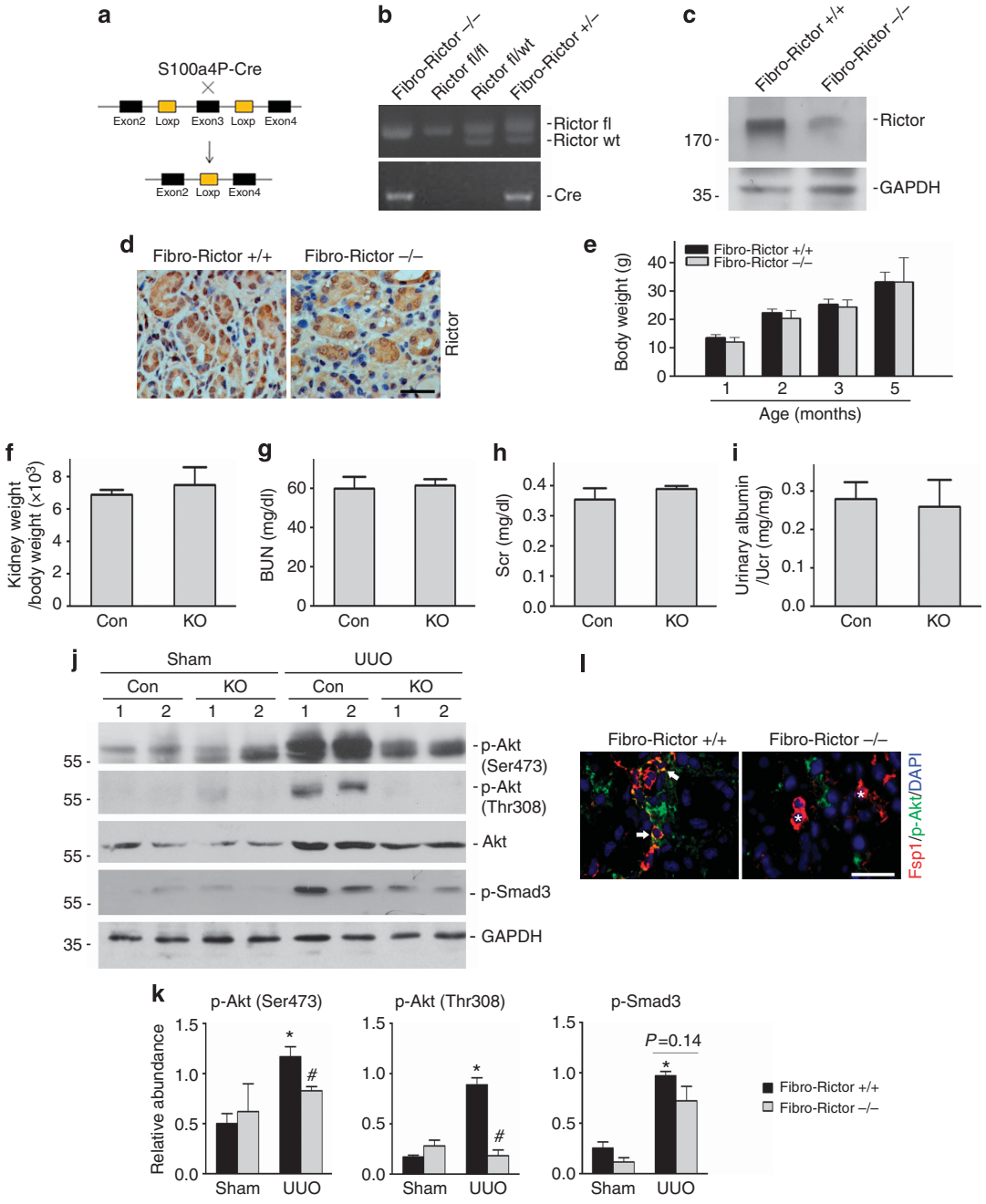

Figure 5 | Generating the mice with fibroblast-specific ablation of the Rictor. (**a**) Diagram illustrates the strategy for generating mice with fibroblast-specific deletion of Rictor. (**b**) Genotyping the mice by PCR analysis of genomic DNA. (**c**) Western blotting analyses showing Rictor protein abundance in the kidney lysates from Fibro-Rictor −/− mice and their control littermates at day 14 after unilateral ureter obstruction (UUO). Kidney lysates were immunoblotted with Abs against Rictor and glyceraldehyde 3-phosphate dehydrogenase (GAPDH), respectively. (**d**) Representative micrographs showing immunohistochemical staining results for Rictor in the kidneys at day 14 after UUO. The kidney tissue was stained with Ab against Rictor. Scale bar = 20 μm. (**e–i**) There was no difference as to body weight (**e**), kidney/body weight (**f**), blood urea nitrogen (BUN) (**g**), serum creatinine (**h**), and urinary albumin level (**i**) between control littermates and Fibro-Rictor −/− mice within 2 months after birth (n = 4-6). (**j**) Western blotting analyses showing the p-Akt (Ser473) abundance in the kidney lysates from Fibro-Rictor −/− mice and their control littermates at day 14 after UUO. Kidney tissue lysates were immunoblotted with Abs against p-Akt (Ser473), p-Akt (Thr308), Akt, p-Smad3, and GAPDH, respectively. (**k**) Graphic presentation showing the relative p-Akt (Ser473), p-Akt (Thr308), and p-Smad3 abundance normalized to Akt or GAPDH, respectively. *P < 0.05 compared with sham controls (n = 3–4); #P < 0.05 compared with control littermates (n = 3–4). (**l**) Representative micrographs showing the immunostaining results for Fsp1 and p-Akt (Ser473) in the kidneys at day 14 after UUO. The kidney tissue was stained with Abs against Fsp1 and p-Akt (Ser473). Arrows indicate Fsp1 and p-Akt (Ser473)-positive cells. Asterisks indicate Fsp1-positive but p-Akt (Ser473)-negative cells in the knockout kidneys. Scale bar = 20 μm.

breeding strategy for generating the knockout mice. Mice with fibroblast-specific ablation of Rictor were named as Fibro-Rictor−/− (Figure 5b, lane 1), whereas age and gender matched Rictor-floxed littermates were considered as controls (Fibro-Rictor+/+, Figure 5b, lane 3). Western blotting analysis and immunostaining were used to examine the expression of Rictor protein in the kidneys. Rictor protein abundance was markedly reduced in the UUO kidneys from Fibro-Rictor−/− mice compared with those from control littermates (Figure 5c and d). All mice were born normal with expected Mendelian frequency. No significant difference was observed in body weight, kidney/body weight ratio, urinary albumin excretion, blood urea nitrogen or serum creatinine level between the knockouts and control littermates within 2 months after birth, respectively (Figure 5e–i). In short, Fibro-Rictor−/− mice were phenotypic normal under physiological condition.

The mice were subjected to UUO and the Akt phosphorylation was analyzed by western blotting assay. As shown in Figure 5j and k, in the UUO kidneys from control littermates, Akt kinase activation exhibited as Akt phosphorylation (Ser473 and Thr308) were largely induced at day 14, whereas in the Fibro-Rictor−/− kidneys p-Akt (Ser473) abundance was much less. In addition, p-Akt (Thr308) was also significantly diminished in the knockout kidneys after UUO. Phosphorylated Smad3 was upregulated in the UUO kidneys from control littermates and was slightly decreased in the knockout kidneys. Double staining of Abs against Fsp1 and p-Akt (Ser473) showed that phosphorylated Akt at Ser473 could be detected in Fsp1-positive cells in the kidneys with UUO nephropathy, whereas p-Akt (Ser473) was negative in Fsp1-positive cells in the knockout kidneys after UUO (Figure 5l). These results suggest that deletion of Rictor in fibroblasts diminishes Akt phosphorylation at Ser473 in the fibroblasts from the UUO kidneys.

Specific deletion of Rictor in fibroblasts ameliorates kidney interstitial fibrosis in mice with UUO nephropathy

The above data demonstrated that deletion of Rictor in fibroblasts diminished Akt kinase phosphorylation in the kidneys with UUO nephropathy. Kidney sections from different groups were stained with periodic acid–Schiff, Masson, or Sirius red. In the sham groups, the kidney morphology was comparable between the knockouts and controls. In the kidneys with UUO nephropathy from control littermates, remarkably tubular atrophy and interstitial extracellular matrix deposition could be found, whereas in the knockout kidneys tubular damage as well as extracellular matrix deposition were largely alleviated (Figure 6a). As shown in Figure 6b, the fibrotic area was largely increased in the control littermates with UUO nephropathy, whereas specific deletion of Rictor in fibroblast could markedly ameliorate kidney fibrosis. The total collagen content within the kidneys was significantly increased at 1 or 2 weeks after UUO from control littermates, and in the knockout kidneys, total collagen content was diminished (Figure 6c).

Fibronectin, α-SMA, and type I collagen expression in the kidneys were also examined by western blotting assay and immunostaining. As shown in Figure 7a and b, FN, α-SMA, and type I collagen protein abundance were remarkably increased after UUO in control littermates, and they were significantly decreased in the knockout kidneys compared with those in the control littermates. immunostaining for FN, α-SMA, and type I collagen further confirmed the results of western blotting assay (Figure 7c). Taken together, these results demonstrate that specific deletion of Rictor in fibroblasts ameliorates fibroblast activation and kidney fibrosis after UUO operation.

Kidney interstitial cell apoptosis is decreased in the knockouts with UUO nephropathy

Our previous study demonstrated that Rictor/mTORC2 signaling has a critical role in protecting against tubular cell death induced by cisplatin treatment.[20] To investigate cell survival status in the UUO kidneys from the knockouts, TUNEL (terminal deoxynucleotidyl transferase-mediated dUTP-fluorescein nick end labeling) staining was employed. As shown in Figure 8a and b, in the sham groups, few TUNEL-positive tubular or interstitial cells could be detected. In the UUO kidneys from control littermates, at day 14 after surgery the number for TUNEL-positive tubular or interstitial cells was significantly increased, while in the UUO kidneys from the knockouts both tubular cell and interstitial cell apoptosis was significantly ameliorated compared with those in the control littermates. These results suggest that fibroblast apoptosis in the knockout kidneys is not exacerbated under physiological condition or after UUO compared with those in control littermates.

Ablation of Rictor in the fibroblasts attenuates macrophage infiltration in kidneys with UUO nephropathy

Kidney interstitial macrophage infiltration is one of the most important features of chronic kidney diseases. To evaluate the macrophage infiltration in the kidneys, immunostaining for F4/80 was employed, and F4/80+ cells were counted in at least five randomly selected fields (×400) for each sample. As shown in Figure 9a and b, few F4/80-positive cells were detected in the sham groups. The number of F4/80-positive cell was significantly increased in the kidneys with UUO nephropathy from control littermates, while in the knockout kidneys macrophage infiltration was much less. We performed co-immunostaining of anti-Fsp1 with anti-α-SMA or with anti-F4/80 on the kidney tissues with UUO nephropathy. Immunofluorescent staining results showed that 73.7% of the Fsp1-positive cells expressed α-SMA; about 16.4% of the Fsp1-postive cells were co-stained with F4/80; and only 5.8% of the F4/80-positive cells were Fsp1 positive (Figure 9c).

DISCUSSION

Fibroblasts are regarded as the principal cells that generate a large amount of matrix components that accumulate within the interstitial space upon activation.[2,27–36] It has been

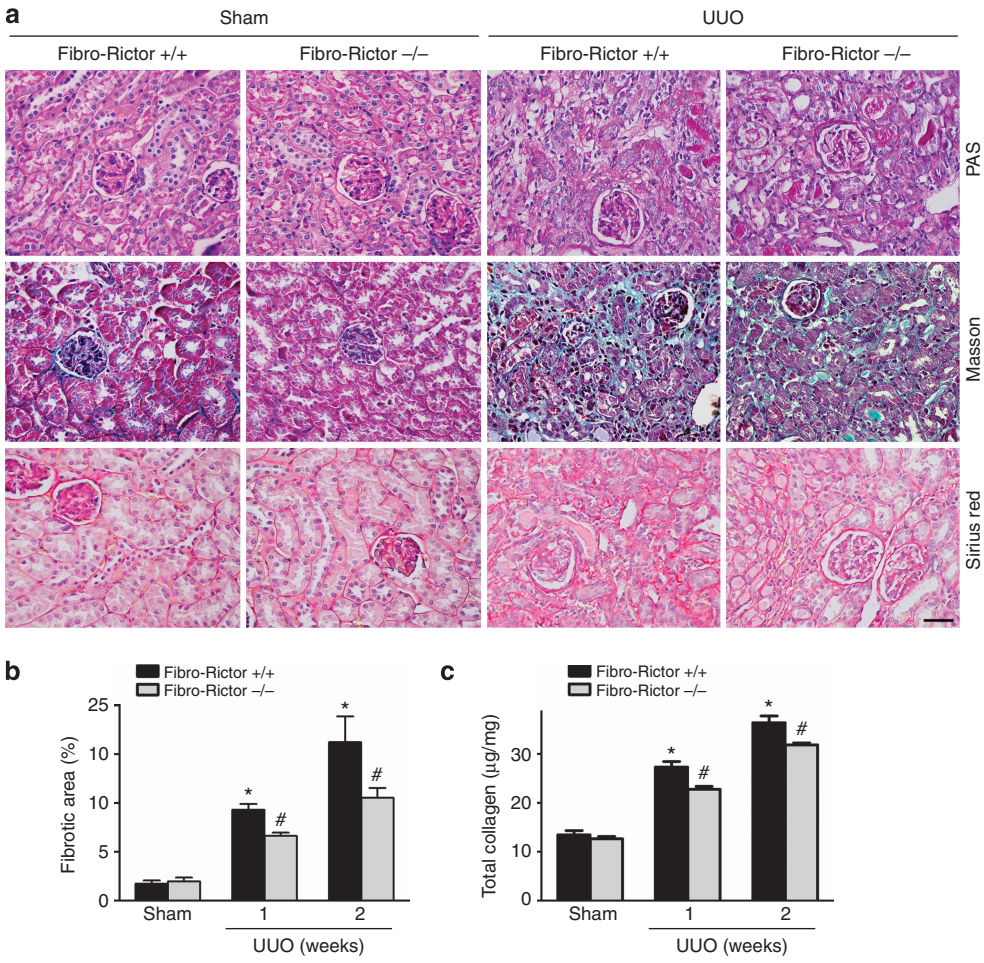

Figure 6 | Specific deletion of Rictor in fibroblasts ameliorates kidney interstitial fibrosis in mice with unilateral ureter obstruction (UUO) nephropathy. The knockouts and control littermates received UUO operation and were killed at 1 or 2 weeks after surgery. (**a**) Representative micrographs for periodic acid–Schiff (PAS), Masson, and Sirius red staining in the kidneys from the different groups as indicated. Scale bar = 20 μm. (**b**) Graphic presentation showing the fibrotic area in the kidneys from the different groups as indicated. $^{*}P<0.05$ compared with sham control ($n=5$); $^{\#}P<0.05$ compared with control littermates with UUO nephropathy ($n=5$). (**c**) Graphic presentation showing total collagen content in the kidneys from different groups as indicated. $^{*}P<0.05$ compared with sham control ($n=5$); $^{\#}P<0.05$ compared with control littermates with UUO nephropathy ($n=5$).

reported that mTORC1 signaling mediates the fibrogenic process through promoting fibroblast activation and kidney interstitial fibrosis.[8,13,37] Here we demonstrated that Rictor/mTORC2 signaling activation contributes to TGFβ1-promoted fibroblast activation independent of mTORC1 signaling.

In cultured NRK-49F cells, TGFβ1 treatment could induce both mTORC1 and mTORC2 signaling activation at a similar pattern and blocking either one of them could partially interfere with TGFβ1-induced fibroblast activation. It may be concluded that the activation of both signaling are required for the full activation of fibroblast after TGFβ1 treatment. In *in vivo* studies, we found that phosphorylated Smad3 was slightly decreased in the knockout kidneys after UUO operation compared with those in the control littermates, which suggest that long-term ablation of mTORC2 may reduce the activity of TGFβ1 itself. However, how does TGFβ1 induce these signaling activation in kidney fibroblasts is not clear?

The crosstalk between two complexes is complicated and seems on a cellular context–dependent manner. MTORC1 may impair the activation of mTORC2 by phosphorylating insulin receptor substrate-1, Grb10, or Sin1.[38–40] Whereas Humphrey *et al.*[41] found that phosphorylation of Thr 86 in Sin1 actually augments mTORC2 activity. MTORC2 may stimulate mTORC1 signaling activation through phosphorylated Akt at Ser473, an activator of mTORC1 through phosphorylation of TSC2. However, in this study, we found that knocking down Rictor expression could not affect TGFβ1-induced S6 phosphorylation, suggesting that the profibrotic role of mTORC2 is independent of mTORC1 signaling in kidney fibroblast (Figure 2b). Because of the overall complexity of the context-dependent regulation and function of the mTOR pathway, and most of the results are

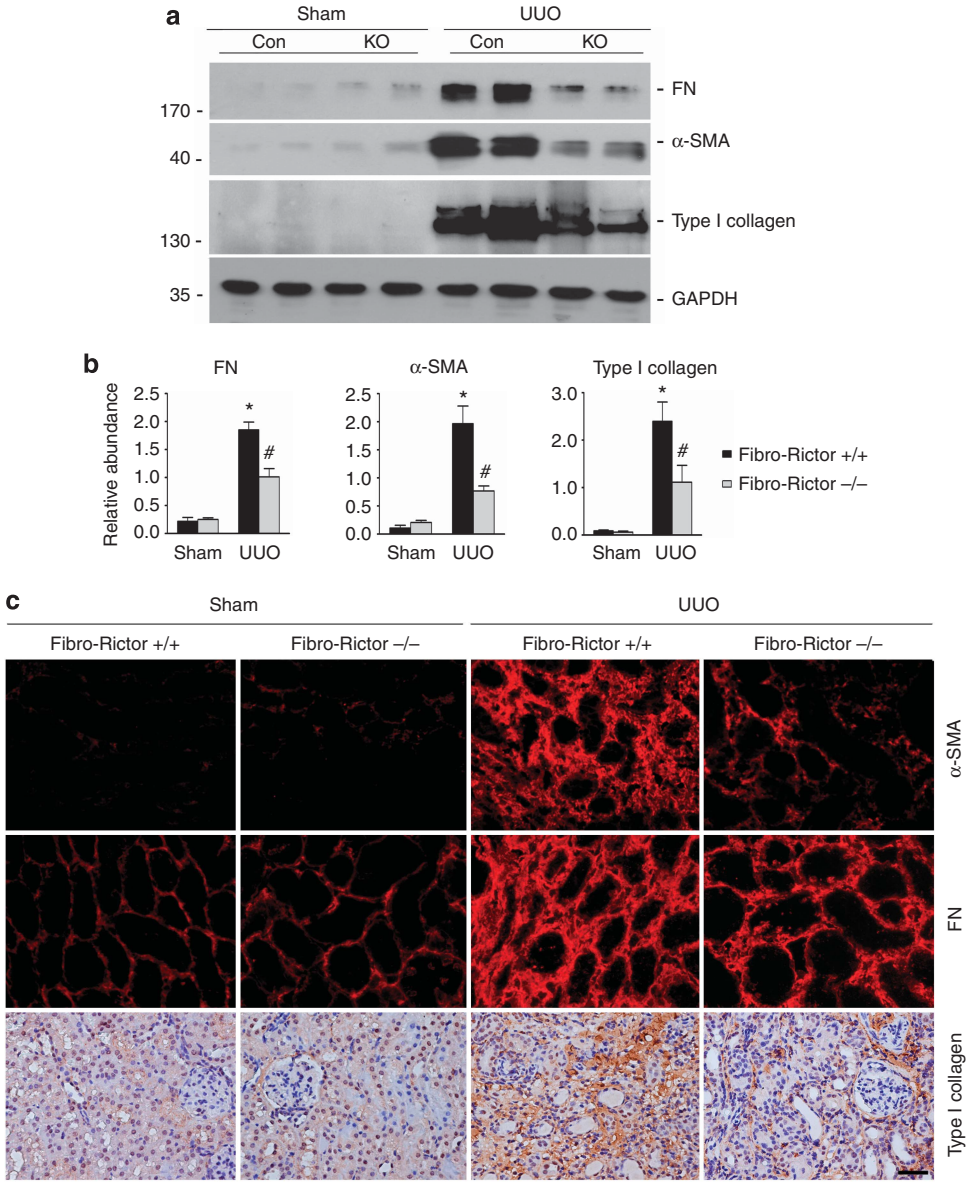

Figure 7 | Specific deletion of Rictor in fibroblasts diminishes fibronectin (FN), α-smooth muscle actin (α-SMA), and type I collagen expression in the unilateral ureter obstruction (UUO) kidneys in mice. (**a**) Western blotting analyses showing FN, α-SMA, and type I collagen expression in the Fibro-Rictor+/+ or Fibro-Rictor−/− kidneys at day 14 after UUO. (**b**) Graphic presentation showing FN, α-SMA, and type I collagen protein abundance in the kidneys from Fibro-Rictor+/+ or Fibro-Rictor−/− kidneys at day 14 after UUO. *$P<0.05$ compared with the sham kidneys ($n=4$); #$P<0.05$ compared with control littermates ($n=4$). (**c**) Representative micrographs showing immunostaining for FN, α-SMA, and type I collagen expression in various groups as indicated. Scale bar = 20 μm.

not obtained from kidney fibroblast, further work is needed to elucidate the interaction between mTORC1 and mTORC2 in kidney fibroblast activation and kidney fibrosis.

Akt kinase controls many fundamental cellular processes, such as cell proliferation and survival.[20,24,42,43] Inhibition of phosphatidylinositol 3′-kinase/Akt signaling may ameliorate UUO nephropathy in mice.[44–46] In the kidneys, Akt1 and Akt2 but not Akt3 can be detected.[23] MTORC2 may regulate the activity of both Akt1 and Akt2.[24,25,47] In this study, downregulating Akt1 could inhibit TGFβ1-induced FN and α-SMA expression, while downregulating Akt2 could only diminish TGFβ1-induced α-SMA expression. Except for Akt, SGK1 phosphorylation was also increased after TGFβ1 treatment. Considering the critical role of SGK1 activation in promoting kidney fibrosis,[48] SGK1 phosphorylation may also contribute to TGFβ1-induced kidney fibroblast activation. It has been reported that Rictor/mTORC2 signaling is important for the regulation of energy and glucose metabolism in many cell types.[17] Whether Rictor/mTORC2 signaling mediating TGFβ1-promoted fibroblast activation is through regulating cellular energy and glucose metabolism needs further investigation.

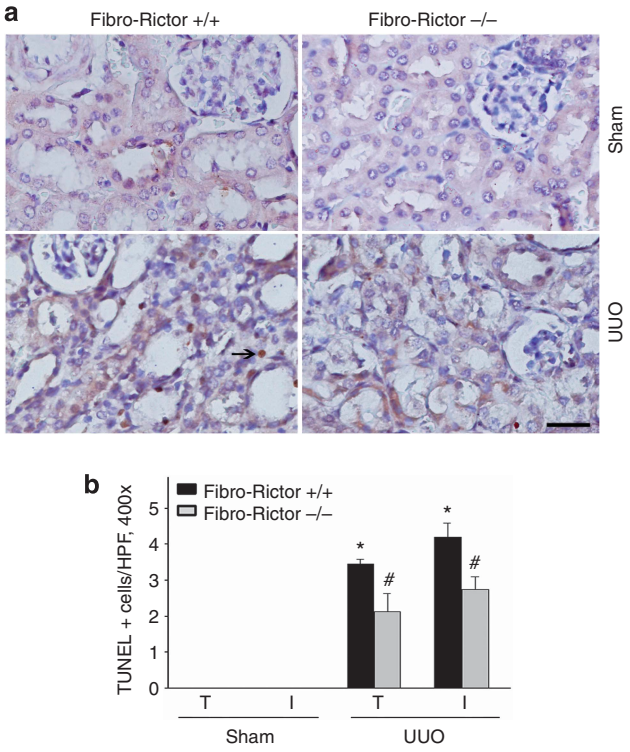

Figure 8 | Cell apoptosis is attenuated in the kidneys from Fibro-Rictor – / – mice with unilateral ureter obstruction (UUO) nephropathy. (**a**) Representative micrographs showing TUNEL (terminal deoxynucleotidyl transferase-mediated dUTP-fluorescein nick end labeling) staining for apoptotic cells among different groups as indicated. Arrow indicates TUNEL-positive interstitial cells. Scale bar = 20 μm. (**b**) Graphic presentation showing TUNEL-positive tubular or interstitial cells in the kidneys from the Fibro-Rictor+/+ or Fibro-Rictor – / – kidneys at day 14 after UUO. *$P < 0.05$ compared with sham control ($n = 3$-4); #$P < 0.05$ compared with control littermates with UUO nephropathy ($n = 4$).

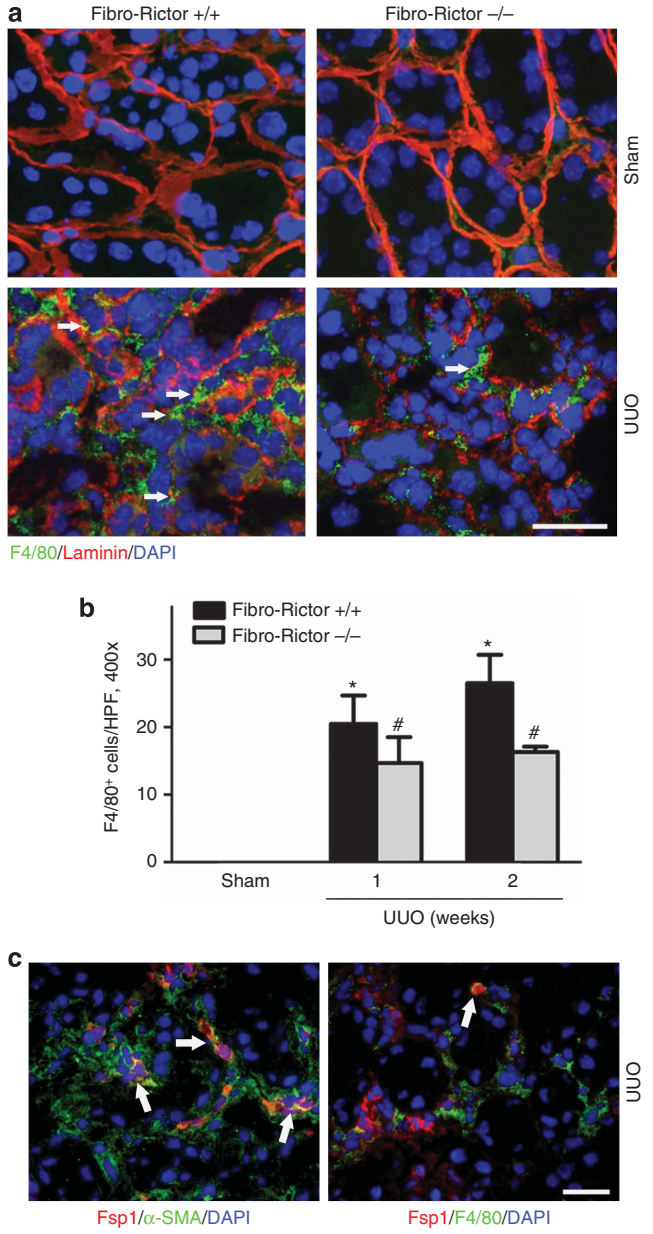

Figure 9 | Macrophage infiltration is diminished in the kidneys from Fibro-Rictor – / – mice with unilateral ureter obstruction (UUO) nephropathy. (**a**) Representative micrographs showing immunofluorescence staining for F4/80 among different groups as indicated. Slides were co-stained with Abs against F4/80 and laminin. Kidney sections were counterstained with DAPI (4,6-diamidino-2-phenylindole) to visualize the cell nuclei. Arrows indicate F4/80-positive macrophage. Scale bar = 20 μm. (**b**) Graphic presentation showing F4/80-positive macrophage infiltration in the kidneys from Fibro-Rictor+/+ or Fibro-Rictor – / – kidneys at day 7 and 14 after UUO. *$P < 0.05$ compared with sham control ($n = 3$-4); #$P < 0.05$ compared with control littermates with UUO nephropathy ($n = 4$). (**c**) Representative micrographs showing the immunostaining of Fsp1 with α-SMA or Fsp1 with F4/80. White arrows indicate co-staining positive cells. Scale bar = 20 μm.

In this study, no obvious phenotypic change could be found within 2 months after birth in mice with fibroblast-specific deletion of Rictor gene, indicating that Rictor/mTORC2 in fibroblast is dispensable under physiological condition *in vivo*. Our previous studies report that Rictor/mTORC2 signaling in tubular cells is protective against cisplatin-induced cell apoptosis and acute kidney injury. However, in this study, both interstitial cell and tubular cell apoptosis were largely decreased in the knockout kidneys after UUO compared with their control littermates. Less kidney injury may account for the less apoptotic tubular or interstitial cells in the knockout kidneys. It is of note here that a paracrine mediator such as miR-34a derived from fibroblast in fibrotic kidneys may induce tubular cell apoptosis.[49] However, whether mTORC2 mediates TGFβ1-induced miR-34a production in fibroblast is not clear.

Interstitial accumulation of macrophages is strongly associated with the progression of renal injury in UUO model.[4,50,51] Fibro-Rictor – / – mice exhibited less macrophage infiltration compared with those in control littermates after UUO. As 5.8% of the macrophages express Fsp1 in the fibrotic kidneys, the function of this portion of the macrophages may be impaired in the knockouts. Less macrophage infiltration in the knockout kidneys may account for three reasons: the first one is that less kidney injury in the

knockouts may lead to decreased macrophage infiltration; the second one is that Rictor/mTORC2 signaling activation in fibroblasts may directly stimulate interstitial inflammation under diseased condition; and the third one is that the deletion of Rictor in some macrophages may impair their function (Figure 9c).

In conclusion, this study demonstrated that Rictor/mTORC2 signaling has an important role in mediating TGFβ1-induced fibroblast activation and kidney fibrosis. Targeting this signaling pathway may provide a new strategy for inhibiting the progression of chronic kidney diseases.

MATERIALS AND METHODS

Mice and animal models

Homozygous Rictor floxed mice (C57BL/6J background) were kindly provided by Dr Magnuson from the University of Vanderbilt.[19] The S100a4-Cre transgenic mice expressing Cre recombinase under the control of the mouse S100a4 promoter were ordered from Jackson Laboratory (012641, C57BL/6J background, The Jackson Laboratory, Bar Harbor, ME). All animals were maintained in the specific pathogen-free Laboratory Animal Center of Nanjing Medical University according to the guidelines of the Institutional Animal Care and Use Committee at Nanjing Medical University, Nanjing, China. By mating Rictor floxed mice with S100a4-Cre transgenic mice, mice that were heterozygous for the Rictor-floxed allele were generated (genotype: Rictor fl/wt, Cre+/−). These mice were crossbred with homozygous Rictor floxed mice (genotype: Rictor fl/fl) to generate offspring with specific deletion of Rictor in the fibroblasts (Fibro-Rictor −/−, genotype: Rictor fl/fl, Cre+/−). The breeding protocol also generated heterozygous littermates (genotype: Rictor fl/wt, Cre+/−) and the other groups of mice (Rictor fl/fl, Cre−/−; Rictor fl/wt). The same gender mice genotyping Rictor fl/fl, Cre−/− from the same litters with the knockouts were considered as control littermates. Genotyping was performed by PCR assay using DNA extracted from the mouse tail. The primers used for genotyping were as follows: Cre transgene, sense: 5′-TTGCCTGCA TTACCGGTCGATGC-3′ and anti-sense: 5′-TTGCACGTTCACC GGCATCAACG-3′; and Rictor genotyping, sense:5′-GACACTGGA TTACAGTGGCTTG-3′ and anti-sense: 5′-GCTGGGCCATCT GAATAACTTC-3′.

Male CD1 mice weighing ~18–22 g were acquired from the specific pathogen-free Laboratory Animal Center of Nanjing Medical University and maintained according to the guidelines of the Institutional Animal Care and Use Committee at Nanjing Medical University. UUO was performed as previously reported.[2] The UUO kidneys were harvested at days 7 and 14 after surgery. One portion of the kidney was fixed in 10% phosphate-buffered formalin, followed by paraffin embedding for histological and immunohistochemical staining. Another portion was immediately frozen in Tissue-Tek optimum cutting temperature compound (Sakura Finetek, Torrance, CA) for cryosection. The remaining kidney tissue was snap-frozen in liquid nitrogen and stored at −80 °C for extraction of RNA and protein.

Cell culture and treatment

Rat kidney interstitial fibroblasts (NRK-49F) cells were obtained from American Type Culture Collection (Manassas, VA). Cells were cultured in Dulbecco's modified Eagle's medium/F12 medium supplemented with 10% fetal bovine serum (Invitrogen, Grand Island, NY). The cells were seeded on six-well culture plates to 60–70% confluence in complete medium containing 10% fetal bovine serum for 16 h and then changed to serum-free medium after washing twice with serum-free medium. Recombinant human TGFβ1 (cat.: 100-B-010-CF, R&D Systems, Minneapolis, MN) was added to the serum-free medium for various periods of time. Rictor or Scramble siRNA (GenePharma, Shanghai, China) was transfected into NRK-49F cells using Lipofectamine 2000 reagent (Invitrogen) according to the manufacturer's instruction.

Urinary albumin, serum creatinine, and blood urea nitrogen assay

Urinary albumin concentration was measured by using a mouse Albumin ELISA Quantification Kit (Bethyl Laboratories, Montgomery, TX). Serum creatinine was measured with the QuantiChrom Creatinine Assay Kit (cat.: DICT-500, Bioassay Systems, Hayward, CA), and blood urea nitrogen was measured with the QuantiChrom Urea Assay Kit (cat.: DIUR-500, Bioassay Systems) according to the manufacturer's instructions.

Histology and immunohistochemistry

Kidney samples were fixed in 10% neutral formalin and embedded in paraffin. Three-μm thick sections were used for periodic acid–Schiff and Masson staining. For immunohistochemical staining, paraffin-embedded kidney sections were deparaffinized, hydrated, and antigen-retrieved, and endogenous peroxidase activity was quenched by 3% H_2O_2. Sections were then blocked with 10% normal donkey serum, followed by incubation with anti-Rictor (cat.: A300-459A, Bethyl Laboratories), or anti-type I collagen (cat.: AB765P, Millipore, Billerica, MA) over night at 4 °C. After incubation with secondary antibody for 1 h, sections were incubated with ABC reagents for 1 h at room temperature before being subjected to substrate 3-amino-9-ethylcarbazole or 3,3′diaminobenzidine (Vector Laboratories, Burlingame, CA). Slides were viewed with a Nikon Eclipse 80i microscope equipped with a digital camera (DS-Ri1, Nikon, Shanghai, China).

Immunofluorescent staining

Kidney cryosections at 3-μm thickness were fixed for 15 min in 4% paraformaldehyde, followed by permeabilization with 0.2% Triton X-100 in phosphate-buffered saline (PBS) for 5 min at room temperature. After blocking with 2% donkey serum for 60 min, the slides were immunostained with anti-FN (cat.: F3648, Sigma-Aldrich, St Louis, MO), anti-α-SMA (cat.: A5228, Sigma-Aldrich), anti-Rictor (cat.: A300-459A, Bethyl Laboratories), anti-F4/80 (cat.: 14–4801, eBioscience, San Diego, CA), anti-p-Akt (Ser473), or anti-Fsp1 (cat.: A511401, Dako, Carpinteria, CA). Cells cultured on coverslips were washed twice with cold 1 × PBS and fixed with cold methanol/acetone (1:1) for 10 min at −20 °C. After three extensive washings with 1 × PBS, the cells were treated with 0.1% TritonX-100 for 5 min and blocked with 2% normal donkey serum in 1 × PBS buffer for 40 min at room temperature and incubated with the Anti-Rictor, anti-FN, or anti-α-SMA, followed by staining with fluorescein isothiocyanate or tetramethylrhodamine-conjugated secondary antibody. Cells were also stained with 4',6-diamidino-2-phenylindole to visualize the nuclei. Slides were viewed with a Nikon Eclipse 80i Epi-fluorescence microscope equipped with a digital camera.

Quantitative determination of collagen in kidney tissue

The kidney tissue collagen was quantitated as previously reported.[52] Briefly, 3-μm-thick sections of paraffin-embedded tissue were

stained with Sirius red F3BA and Food Green FCF (Sigma-Aldrich) overnight. After washing three times with 1 × PBS buffer, the dye was eluted from tissue sections with 0.1 N sodium hydroxide methanol. Absorbance at 540 and 605 nm were determined for Sirius red F3BA and Food Green FCF-binding protein, respectively. This assay provides a simple, relative measurement of the ratio of collagen to total protein, which is expressed as micrograms per milligram of total protein. As to the quantification of fibrotic area, kidney section with Masson trichrome staining was used, and five randomly selected fields for each animal under × 400 microscope were quantified. The percentage of Masson-stained positive area was calculated using the Image J software (NIH, Besthesda, MD). Five individual animals for each group were used for matrix quantification.

Western blotting analysis

Cultural NRK-49F cells were lysed in 1 × sodium dodecyl sulfate sample buffer. The kidneys were lysed with radioimmunoprecipitation assay solution containing 1% NP40, 0.1% sodium dodecyl sulfate, 100 mg/ml phenylmethanesulfonylfluoride, 1% protease inhibitor cocktail, and 1% phosphatase I and II inhibitor cocktail (Sigma, St Louis, MO) on ice. The supernatants were collected after centrifugation at 13,000 × *g* at 4 °C for 30 min. Protein concentration was determined by bicinchoninic acid protein assay (BCA Kit; Pierce Thermo-Scientific, Rockford, IL) according to the manufacturer's instructions. An equal amount of protein was loaded into 10 or 12% sodium dodecyl sulfate-polyacrylamide gel electrophoresis and transferred onto polyvinylidene difluoride membranes. The primary antibodies were as follows: anti-Rictor (cat.: ab70374, Abcam, Cambridge, MA) or anti-Rictor (cat.: A300-459A, Bethyl Laboratories), anti-GAPDH (anti-glyceraldehyde 3-phosphate dehydrogenase; cat.: FL-335, Santa Cruz Biotechnology, Dallas, TX), anti-p-Akt (ser473) (cat.: 3868, Cell Signaling Technology, Shanghai, China), anti-p-Akt (Thr308) (cat.: 2965, Cell Signaling Technology), anti-Akt (cat.: 4691, Cell Signaling Technology), anti-p-SGK1 (Ser422) (cat.: ab55281, Abcam), anti-p-Smad3 (Ser423/425) (cat.: ab52903, Abcam), anti-Akt1 (cat.: 2938, Cell Signaling Technology), anti-Akt2 (cat.: 2964, Cell Signaling Technology, anti-p-PKCα (Thr638/641) (cat.: 9375, Cell Signaling Technology), anti-PKCα (cat.: 2056, Cell Signaling Technology), anti-FN (cat.: F3648, Sigma-Aldrich), anti-α-SMA (cat.: A5228, Sigma-Aldrich), and anti-type I collagen (cat.: AB765P, Millipore). Quantification was performed by measuring the intensity of the signals with the aid of National Institutes of Health Image J software package.

RNA isolation and real-time quantitative reverse transcriptase–PCR

Total RNA was extracted using Trizol reagent (Invitrogen) according to the manufacturer's instructions. cDNA was synthesized with 1 μg of total RNA, ReverTra Ace (Vazyme, Nanjing, China), and oligo (dT) 12–18 primers. Gene expression was measured by real-time PCR assay (Vazyme) and 7300 real-time PCR system (Applied Biosystems, Foster City, CA). The relative amount of mRNA or gene to internal control was calculated using the equation $2^{\triangle CT}$, in which $\triangle CT = CT_{gene} - CT_{control}$.

Statistical analysis

All data examined are presented as mean ± s.e.m. Statistical analysis of the data was performed using the SigmaStat software (Jandel Scientific Software, San Rafael, CA). Comparison between groups was made using one-way analysis of variance, followed by the Student–Newman–Keuls test. $P < 0.05$ was considered statistically significant.

DISCLOSURE

All the authors declared no competing interests.

ACKNOWLEDGMENTS

This work was supported by the National Basic Research Program of China 973 program (2012CB517601) and Science Foundation of Jiangsu Province Grants BK20140048 to CD.

SUPPLEMENTARY MATERIAL

Figure S1. Knocking down Rictor expression does not affect TGFβ1-Induced smad3 phosphorylation.

Figure S2. Knocking down Akt diminishes TGFβ1-induced fibroblast activation.

Supplementary material is linked to the online version of the paper at http://www.nature.com/ki

REFERENCES

1. Sharma SK, Zou H, Togtokh A *et al.* Burden of CKD, proteinuria, and cardiovascular risk among Chinese, Mongolian, and Nepalese participants in the International Society of Nephrology screening programs. *Am J Kidney Dis* 2010; **56**: 915–927.
2. Liu Y. Cellular and molecular mechanisms of renal fibrosis. *Nat Rev Nephrol* 2011; **7**: 684–696.
3. Duffield JS. Cellular and molecular mechanisms in kidney fibrosis. *J Clin Invest* 2014; **124**: 2299–2306.
4. Boor P, Ostendorf T, Floege J. Renal fibrosis: novel insights into mechanisms and therapeutic targets. *Nat Rev Nephrol* 2010; **6**: 643–656.
5. Johnson SC, Rabinovitch PS, Kaeberlein M. mTOR is a key modulator of ageing and age-related disease. *Nature* 2013; **493**: 338–345.
6. Delgoffe GM, Pollizzi KN, Waickman AT *et al.* The kinase mTOR regulates the differentiation of helper T cells through the selective activation of signaling by mTORC1 and mTORC2. *Nat Immunol* 2011; **12**: 295–303.
7. Laplante M, Sabatini DM. mTOR signaling at a glance. *J Cell Sci* 2009; **122**: 3589–3594.
8. Inoki K. Role of TSC-mTOR pathway in diabetic nephropathy. *Diabetes Res Clin Pract* 2008; **82**: S59–S62.
9. Mori H, Inoki K, Masutani K *et al.* The mTOR pathway is highly activated in diabetic nephropathy and rapamycin has a strong therapeutic potential. *Biochem Biophys Res Commun* 2009; **384**: 471–475.
10. Lieberthal W, Fuhro R, Andry C *et al.* Rapamycin delays but does not prevent recovery from acute renal failure: role of acquired tubular resistance. *Transplantation* 2006; **82**: 17–22.
11. Lieberthal W, Fuhro R, Andry CC *et al.* Rapamycin impairs recovery from acute renal failure: role of cell-cycle arrest and apoptosis of tubular cells. *Am J Physiol Renal Physiol* 2001; **281**: F693–F706.
12. Grahammer F, Haenisch N, Steinhardt F *et al.* mTORC1 maintains renal tubular homeostasis and is essential in response to ischemic stress. *Proc Natl Acad Sci USA* 2014; **111**: E2817–E2826.
13. Jiang L, Xu L, Mao J *et al.* Rheb/mTORC1 signaling promotes kidney fibroblast activation and fibrosis. *J Am Soc Nephrol* 2013; **24**: 1114–1126.
14. Goc A, Choudhary M, Byzova TV *et al.* TGFbeta- and bleomycin-induced extracellular matrix synthesis is mediated through Akt and mammalian target of rapamycin (mTOR). *J Cell Physiol* 2011; **226**: 3004–3013.
15. Cybulski N, Hall MN. TOR complex 2: a signaling pathway of its own. *Trends Biochem Sci* 2009; **34**: 620–627.
16. Goncharova EA, Goncharov DA, Li H *et al.* mTORC2 is required for proliferation and survival of TSC2-null cells. *Mol Cell Biol* 2011; **31**: 2484–2498.
17. Kocalis HE, Hagan SL, George L *et al.* Rictor/mTORC2 facilitates central regulation of energy and glucose homeostasis. *Mol Metab* 2014; **3**: 394–407.
18. Facchinetti V, Ouyang W, Wei H *et al.* The mammalian target of rapamycin complex 2 controls folding and stability of Akt and protein kinase C. *EMBO J* 2008; **27**: 1932–1943.
19. Gu Y, Lindner J, Kumar A *et al.* Rictor/mTORC2 is essential for maintaining a balance between beta-cell proliferation and cell size. *Diabetes* 2011; **60**: 827–837.
20. Li J, Xu Z, Jiang L *et al.* Rictor/mTORC2 protects against cisplatin-induced tubular cell death and acute kidney injury. *Kidney Int* 2014; **86**: 86–102.

21. Lamouille S, Connolly E, Smyth JW *et al.* TGF-beta-induced activation of mTOR complex 2 drives epithelial-mesenchymal transition and cell invasion. *J Cell Sci* 2012; **125**: 1259–1273.
22. Chang W, Wei K, Ho L *et al.* A critical role for the mTORC2 pathway in lung fibrosis. *PLoS One* 2014; **9**: e106155.
23. Tschopp O, Yang ZZ, Brodbeck D *et al.* Essential role of protein kinase B gamma (PKB gamma/Akt3) in postnatal brain development but not in glucose homeostasis. *Development* 2005; **132**: 2943–2954.
24. Kim EK, Yun SJ, Ha JM *et al.* Selective activation of Akt1 by mammalian target of rapamycin complex 2 regulates cancer cell migration, invasion, and metastasis. *Oncogene* 2011; **30**: 2954–2963.
25. Canaud G, Bienaime F, Viau A *et al.* AKT2 is essential to maintain podocyte viability and function during chronic kidney disease. *Nat Med* 2013; **19**: 1288–1296.
26. Yang J, Dai C, Liu Y. Hepatocyte growth factor suppresses renal interstitial myofibroblast activation and intercepts Smad signal transduction. *Am J Pathol* 2003; **163**: 621–632.
27. Eddy AA. Molecular insights into renal interstitial fibrosis. *J Am Soc Nephrol* 1996; **7**: 2495–2508.
28. Humphreys BD, Lin SL, Kobayashi A *et al.* Fate tracing reveals the pericyte and not epithelial origin of myofibroblasts in kidney fibrosis. *Am J Pathol* 2010; **176**: 85–97.
29. LeBleu VS, Taduri G, O'Connell J *et al.* Origin and function of myofibroblasts in kidney fibrosis. *Nat Med* 2013; **19**: 1047–1053.
30. Liu Y. New insights into epithelial-mesenchymal transition in kidney fibrosis. *J Am Soc Nephrol* 2010; **21**: 212–222.
31. Wada T, Sakai N, Matsushima K *et al.* Fibrocytes: a new insight into kidney fibrosis. *Kidney Int* 2007; **72**: 269–273.
32. Wynn TA. Cellular and molecular mechanisms of fibrosis. *J Pathol* 2008; **214**: 199–210.
33. Yang L, Besschetnova TY, Brooks CR *et al.* Epithelial cell cycle arrest in G2/M mediates kidney fibrosis after injury. *Nat Med* 2010; **16**: 535–543.
34. Zeisberg EM, Potenta SE, Sugimoto H *et al.* Fibroblasts in kidney fibrosis emerge via endothelial-to-mesenchymal transition. *J Am Soc Nephrol* 2008; **19**: 2282–2287.
35. Zeisberg M, Bonner G, Maeshima Y *et al.* Renal fibrosis: collagen composition and assembly regulates epithelial-mesenchymal transdifferentiation. *Am J Pathol* 2001; **159**: 1313–1321.
36. Zeisberg M, Neilson EG. Mechanisms of tubulointerstitial fibrosis. *J Am Soc Nephrol* 2010; **21**: 1819–1834.
37. Godel M, Hartleben B, Herbach N *et al.* Role of mTOR in podocyte function and diabetic nephropathy in humans and mice. *J Clin Invest* 2011; **121**: 2197–2209.
38. Hsu PP, Kang SA, Rameseder J *et al.* The mTOR-regulated phosphoproteome reveals a mechanism of mTORC1-mediated inhibition of growth factor signaling. *Science* 2011; **332**: 1317–1322.
39. Yu Y, Yoon SO, Poulogiannis G *et al.* Phosphoproteomic analysis identifies Grb10 as an mTORC1 substrate that negatively regulates insulin signaling. *Science* 2011; **332**: 1322–1326.
40. Liu P, Gan W, Inuzuka H *et al.* Sin1 phosphorylation impairs mTORC2 complex integrity and inhibits downstream Akt signalling to suppress tumorigenesis. *Nat Cell Biol* 2013; **15**: 1340–1350.
41. Humphrey SJ, Yang G, Yang P *et al.* Dynamic adipocyte phosphoproteome reveals that Akt directly regulates mTORC2. *Cell Metab* 2013; **17**: 1009–1020.
42. Brunet A, Bonni A, Zigmond MJ *et al.* Akt promotes cell survival by phosphorylating and inhibiting a Forkhead transcription factor. *Cell* 1999; **96**: 857–868.
43. Sarbassov DD, Guertin DA, Ali SM *et al.* Phosphorylation and regulation of Akt/PKB by the rictor-mTOR complex. *Science* 2005; **307**: 1098–1101.
44. Grande MT, Lopez-Novoa JM. Fibroblast activation and myofibroblast generation in obstructive nephropathy. *Nat Rev Nephrol* 2009; **5**: 319–328.
45. Rodriguez-Pena AB, Grande MT, Eleno N *et al.* Activation of Erk1/2 and Akt following unilateral ureteral obstruction. *Kidney Int* 2008; **74**: 196–209.
46. Lan A, Du J. Potential role of Akt signaling in chronic kidney disease. *Nephrol Dial Transplant* 2014; **30**: 385–394.
47. Hresko RC, Mueckler M. mTOR.RICTOR is the Ser473 kinase for Akt/protein kinase B in 3T3-L1 adipocytes. *J Biol Chem* 2005; **280**: 40406–40416.
48. Artunc F, Lang F. Mineralocorticoid and SGK1-sensitive inflammation and tissue fibrosis. *Nephron Physiol* 2014; **128**: 35–39.
49. Zhou Y, Xiong M, Niu J *et al.* Secreted fibroblast-derived miR-34a induces tubular cell apoptosis in fibrotic kidney. *J Cell Sci* 2014; **127**: 4494–4506.
50. Anders HJ, Ryu M. Renal microenvironments and macrophage phenotypes determine progression or resolution of renal inflammation and fibrosis. *Kidney Int* 2011; **80**: 915–925.
51. Grande MT, Perez-Barriocanal F, Lopez-Novoa JM. Role of inflammation in tubulo-interstitial damage associated to obstructive nephropathy. *J Inflamm (Lond)* 2010; **7**: 19.
52. Lopez-De Leon A, Rojkind M. A simple micromethod for collagen and total protein determination in formalin-fixed paraffin-embedded sections. *J Histochem Cytochem* 1985; **33**: 737–743.